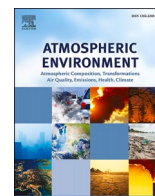




Contents lists available at ScienceDirect

Atmospheric Environment

journal homepage: www.elsevier.com/locate/atmosenv

Effects of ground-level ozone pollution on yield and economic losses of winter wheat in Henan, China

Tuanhui Wang^{a,c,1}, Lin Zhang^{a,c}, Shenghui Zhou^{a,b}, Tianning Zhang^{b,c,1}, Shiyan Zhai^{a,b}, Zhongling Yang^d, Dong Wang^d, Hongquan Song^{a,b,*}

^a Laboratory of Geospatial Technology for the Middle and Lower Yellow River Regions, Ministry of Education, Henan University, Kaifeng, Henan, 475004, China

^b Henan Key Laboratory of Integrated Air Pollution Control and Ecological Security, Henan University, Kaifeng, Henan, 475004, China

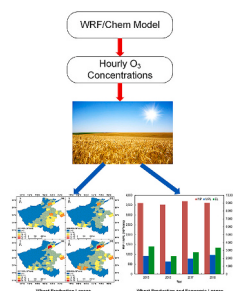
^c Institute of Urban Big Data, College of Geography and Environmental Science, Henan University, Kaifeng, Henan, 475004, China

^d School of Life Sciences, Henan University, Kaifeng, Henan, 475004, China

HIGHLIGHTS

- Spatiotemporal variations of O₃ concentrations in Henan were simulated by WRF/Chem.
- O₃ concentrations and AOT40 showed a clearly increasing trend in most all counties.
- O₃ exposure induced around 14% of total wheat production losses during 2015–2018.

GRAPHICAL ABSTRACT



ARTICLE INFO

Keywords:

AOT40
WRF/Chem
Crop damage
Wheat yield
Food security

ABSTRACT

Ground-level ozone (O₃) is a secondary air pollutant and has negative effects on crops, especially in China in recent years due to the sharply increasing precursors of O₃. Based on the hourly O₃ concentrations simulated by Weather Research and Forecasting model coupled with Chemistry (WRF/Chem) and AOT40 index (accumulation of hourly ozone concentrations exceed 0.04 ppm), we assessed the losses of yield and economy of winter wheat during 2015–2018 at the county level for a central province (Henan) of China. The O₃ concentration and AOT40 during the wheat growing seasons (75-days, 44 days before and 30 days after mid-anthesis) showed a clearly increasing trend over nearly all counties. The annual mean AOT40 was 6.25 ppm h, 4.32 ppm h, 5.26 ppm h, and 6.87 ppm h from 2015 to 2018, respectively. The AOT40 and the loss of relative yield of winter wheat showed significant spatial and temporal variations at the county level. The annual mean relative yield loss of wheat for Henan during 2015–2018 was 12.8%, 8.8%, 10.8%, and 14.1%, respectively, and associated with 2140.10 million, 1318.57 million, 1683.03 million, and 2161.22 million US dollars, respectively. Results indicated that we should formulate more reasonable and stringent emission reduction measures to reduce the O₃ pollution levels and ensure food security in China.

* Corresponding author. College of Geography and Environmental Science, Henan University Jinming Campus, Kaifeng, Henan Province, 475004, China.

E-mail address: hqsong@henu.edu.cn (H. Song).

¹ These authors contributed equally to this work.

<https://doi.org/10.1016/j.atmosenv.2021.118654>

Received 26 January 2021; Received in revised form 5 July 2021; Accepted 2 August 2021

Available online 5 August 2021

1352-2310/© 2021 Elsevier Ltd. All rights reserved.

1. Introduction

Ground-level ozone (O_3) is a secondary air pollutant produced by nitrogen oxides (NOx) and volatile organic compounds (VOCs) under photochemical reactions (Guo et al., 2019; Wang et al., 2019; Liu et al., 2020), which has adverse impacts on climate, air quality, ecosystem, and human health (McGrath et al., 2015; Lin et al., 2018; Zhao et al., 2018; Feng et al., 2019a, 2019b; Guarin et al., 2019). The emission of O_3 precursors (NOx and VOCs) in China had increased sharply over the past three decades due to the rapid increase in the consumption of fossil fuels, resulting in the O_3 pollution level of China surpassing that of North America and Europe (Wang et al., 2017; Li et al., 2020; Liu et al., 2020). High pollution levels of O_3 has long been a major air quality issue in the world, especially the Northern Hemisphere, and the trend is getting worse (Mills et al., 2018a; Lu et al., 2018; Gaudel et al., 2020). Ozone enters plants through stomatal gas exchange, causing damage to plant tissue, such as leaf senescence and shedding, growth and yield reduction, and biotic and abiotic stresses (Wilkinson et al., 2012; Broberg et al., 2015; Feng et al., 2015; Singh and Agrawal, 2016; Mills et al., 2018b; Pleijel et al., 2018).

Over the past few decades, many manipulative experiments based on open top chambers (OTC) systems and free air controlled exposure (FACE) conducted in Europe, America, and Asia have shown that current high levels of O_3 pollution already pose a severe threat to world food production (Massman et al., 2000; Musselman et al., 2006; Wang et al., 2007; Feng and Kobayashi, 2009; Yamaguchi et al., 2014; Feng et al., 2015; Watanabe et al., 2016). On the basis of these experiments, several O_3 exposure metrics have been developed to evaluate the impacts of past, current, and future O_3 pollution levels on the relative yield loss (RYL) of crops at global, national, and regional scales (Avnery et al.,

2011a, 2011b; Danh et al., 2016; Zhao et al., 2018). For instance, AOT40 (accumulation of hourly ozone concentrations exceed 0.04 ppm) (Fuhrer et al., 1997), M7/M12 (mean 7 h or 12 h daytime O_3 concentration) (Adams et al., 1989), SUM06 (accumulated O_3 concentration above the level of 0.06 ppm) (Danh et al., 2016), PODy (phytotoxic ozone dose over a threshold of $y \text{ nmol m}^{-2} \text{ s}^{-1}$) (Mills et al., 2011; Grunhage et al., 2012) etc. Among these O_3 exposure indices, AOT40 is the most commonly used exposure-based metric over the past two decades because it is easy to calculate and has been found to have a strong correlation with RYL of many crops (Mills et al., 2007; Liu et al., 2009; Wang et al., 2012; Zhu et al., 2015; Li et al., 2018).

The AOT40 metric and several response functions of RYL caused by the high O_3 concentration exposure were proposed from local field experiments in Europe (Mills et al., 2007). Several previous studies have adopted response functions based on AOT40 to assess the global, regional, and local effects of surface O_3 exposure on worldwide yields of crops (Mills et al., 2007; Sinha et al., 2015; Zhu et al., 2015; Sicard et al., 2017). However, these response functions were often adopted to estimate the O_3 -induced crop losses in other countries (Amin, 2014; Debaje, 2014; Zhu et al., 2015; Lal et al., 2017). For instance, Avnery et al. (2011b) reported that the yield loss of the world resulted from O_3 pollution ranged from 3.9% to 15.4% for wheat, 8.5–14% for soybean, and 2.2–5.5% for maize in 2000, and projected that wheat relative yield loss (WRYL) of 4.0–26.0%, soybean relative yield loss of 9.5–19.0%, and maize relative yield loss of 2.5–8.7% in 2030 based on atmospheric chemistry transport model and AOT40 response functions (Avnery et al., 2011a). In the United States, the ground-level ozone exposure resulted in 6.7% and 4.9% yield losses for soybean and wheat, respectively, based on the GEOS-Chem model and the AOT40 metric (Lapina et al., 2016). Ghude et al. (2014) concluded that the high O_3 level resulted in $3.5 \pm$

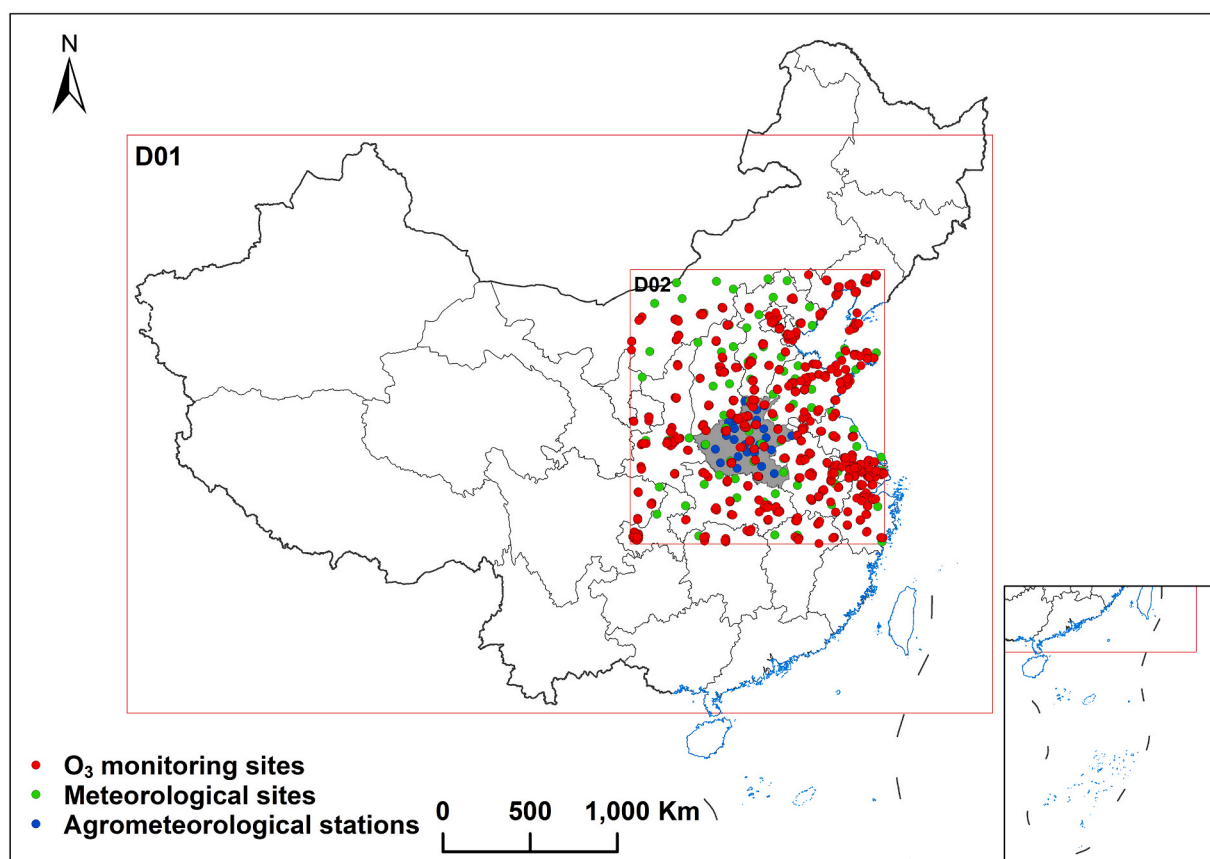


Fig. 1. Map of the WRF/Chem model domain configuration and observation sites. D01 and D02 denote domain 1 and domain 2, respectively. Red, green, and blue points are air quality, meteorological, and agrometeorological observation sites, respectively. The gray shaded area is Henan province of China. (For interpretation of the references to colour in this figure legend, the reader is referred to the Web version of this article.)

Table 1
Configurations of main physical and chemical schemes of the WRF/Chem model.

	Options	Domain 1	Domain 2
Physics	Microphysics	Lin et al.	Lin et al.
	Longwave radiation	New Goddard	New Goddard
	Shortwave radiation	Goddard	Goddard
	Planetary boundary layer	MYJ	MYJ
	Cumulus parameterization	GF	GF
	Land-surface	Noah	Noah
Chemistry	Gas phase chemistry	CBM-Z	CBM-Z
	Aerosol	MOSAIC	MOSAIC
	Photolysis	Madronich F-TUV	Madronich F-TUV
	Aerosol feedback	Open	Open

0.8×10^6 metric tons wheat and $2.1 \pm 0.8 \times 10^6$ metric tons rice losses during the first decade of this century in India, which can sufficiently feed around 35% of 270 million below poverty line population of India (Ghude et al., 2014).

China is a very large country and agriculture is vitally important for this country because it feeds 1.4 billion people or around 19% of the world population (Dong et al., 2020). Wheat, rice, and maize are the three major crops, accounting for more than 95% of China's total food production (Zhai et al., 2021). Accelerated urbanization and industrialization in China have been accompanied by severe air pollution problems characterized by high concentrations of the particulate matter with an aerodynamic diameter less than $2.5 \mu\text{m}$ ($\text{PM}_{2.5}$) and O_3 (Liu et al., 2010; Tang et al., 2013; Wang et al., 2020; Zhang et al., 2021), especially in regions of the Pearl River Delta (PRD), the Yangtze River Delta (YRD), and the North China Plain (NCP) (Feng et al., 2015; Wang et al., 2017; Cheng et al., 2018). Recently, several studies indicated that the $\text{PM}_{2.5}$ concentration has obviously reduced under the execution of the "Action Plan" from 2013 (Cai et al., 2017; Li et al., 2019; Liu et al., 2020; Zhao et al., 2020). However, the reduction of $\text{PM}_{2.5}$ may lead to an increase in the ground level O_3 by enhancing the intensity of photochemical reactions (Lu et al., 2018; Liu et al., 2020; Zhao et al., 2020). Numerous recent studies have found that the ground-level O_3 pollution has surpassed the damage threshold of crops in most regions of China (Lin et al., 2018; Feng et al., 2019b; Zhao et al., 2020). To estimate impacts of surface O_3 pollution on crop productions, several studies have reported national or regional O_3 -caused yield losses of crop in China by using ozone observations or atmospheric chemistry transport models (Avnery et al., 2011a, 2011b; Li et al., 2018; Lin et al., 2018; Zhao et al., 2018; Feng et al., 2019a). However, the O_3 observation sites are mainly located in urban areas, which may intensify uncertainties of the estimation in the O_3 -induced crop yield losses. This is because there are great differences in ozone concentrations between urban and rural/suburban regions and crops mainly distributed in rural/suburban areas (Dueñas et al., 2004; Xu et al., 2011; Guerreiro et al., 2014; Sicard et al., 2016, 2017). Although the atmospheric chemistry transport model can capture the spatiotemporal variations of O_3 concentrations in urban and rural/suburban regions, this kind of studies is scarce in China and the simulations have large uncertainties due to the resolution and accuracy of anthropogenic emission inventories.

On the basis of the above concerns, the hourly O_3 concentration data used in this study were simulated based on the Weather Research and Forecasting model couple with Chemistry (WRF/Chem) during wheat growing seasons in Henan (the major area of crop production in China and is experiencing severe O_3 pollution). The main objectives of this study were to understand the spatiotemporal variations of the ground-level ozone concentration and AOT40 during growing seasons of winter wheat, and to estimate the yield and economic losses for winter wheat induced by O_3 exposure at the county level in Henan in recent years.

2. Materials and methods

2.1. WRF/Chem model configuration

WRF/Chem is a Weather Research and Forecasting (WRF) model coupled with Chemistry (Song et al., 2017; Yu et al., 2021), which can simulate the emission, transport, mixing, and chemical transformation of aerosols and trace gases simultaneously with the meteorological conditions. WRF/Chem (version 3.8.1) was used to simulate hourly ground-level O_3 concentrations during February–June from 2015 to 2018, because the period is the main growing season of winter wheat in Henan province, China. To minimize the effects of initial conditions on simulation results, a spin-up period of one week was conducted for each simulation. The simulation was conducted with a horizontal resolution of $27 \text{ km} \times 27 \text{ km}$ (Domain 1, Fig. 1) and 28 vertical levels from the surface up to 100 hPa. Two-way nesting with horizontal resolution of $9 \text{ km} \times 9 \text{ km}$ (Domain 2, Fig. 1) was adopted over Henan and surrounding areas. Both model domains were projected on the Lambert conformal grid (Domain 1: 185×128 grid points; Domain 2: 166×184 grid points).

Table 1 shows the major physical and chemical options of WRF/Chem in this study. The physical options include Lin et al. microphysics scheme (Lin et al., 1983), the New Goddard longwave (Chou and Suarez, 1999) and Goddard shortwave (Chou and Suarez, 1994) radiation schemes, the Mellor-Yamada-Janjic (MYJ) Planetary Boundary Layer scheme (Janjic, 1994), the Grell-Freitas (GF) cumulus scheme (Grell et al., 2013), and the Noah land surface model (Chen and Dudhia, 2001). The Carbon-Bond Mechanism version Z (CBM-Z) (Zaveri and Peters, 1999) was used as the gas-phase chemistry mechanism in this study. The Model for Simulating Aerosol Interaction and Chemistry (MOSAIC) with 4 sectional aerosol bins including aqueous reactions (Zaveri et al., 2008) was adopted as the aerosol scheme. The Madronich F-TUV photolysis scheme was selected for the photolytic rate calculation (Madronich, 1987).

2.2. WRF/Chem model inputs

The boundary and meteorological initial conditions of WRF/Chem were initialized by using the National Center for Environmental Prediction (NCEP) Final Analysis (FNL) reanalysis datasets with horizontal resolution of $1^\circ \times 1^\circ$ and were available every 6 h. The Community Atmosphere Model with Chemistry (CAM-Chem) (Lamarque et al., 2012; Tilmes et al., 2015), a component of the National Center for Atmospheric Research (NCAR) Community Earth System Model (CESM), datasets were adopted as the initialized chemical and aerosol boundary conditions. The CAM-Chem outputs have a horizontal resolution of $0.9^\circ \times 1.25^\circ$ with 56 vertical levels and are available at every 6 h.

The anthropogenic emissions were generated based on the monthly average Multi-resolution Emission Inventory for China (MEIC) developed by Tsinghua University, China, including emissions of organic carbon (OC), black carbon (BC), carbon monoxide (CO), ammonia (NH_3), sulfur dioxide (SO_2), NOx, VOCs, $\text{PM}_{2.5}$, and the particulate matter with an aerodynamic diameter less than $10 \mu\text{m}$ (PM_{10}) from sectors of power, residential, transportation, industry, and agriculture (Zhang et al., 2009). The biogenic emissions were calculated by using the Model of Emissions of Gas and Aerosols from Nature (MEGAN) (Guenther et al., 2006). The biomass ignition emission data was obtained from Fire Inventory from NCAR (FINN) (Wiedinmyer et al., 2014).

2.3. Observational datasets and evaluation protocols

The performance of meteorological data simulation can directly affect the simulation accuracy of air pollutants due to WRF/Chem simultaneously couples the meteorological simulations online with the atmospheric chemistry (Song et al., 2017). We adopted the 3-h in situ

Table 2
Quantitative statistical indices used in the model performance evaluation (modified from Zhang et al., 2006).

Metrics	Mathematical Formula	Range
Mean Bias (MB)	$MB = \frac{1}{N} \sum_{i=1}^N (M_i - O_i)$	$[-\infty, +\infty]$
Normalized Mean Bias (NMB)	$NMB = \frac{\sum_{i=1}^N (M_i - O_i)}{\sum_{i=1}^N O_i}$	$[-1, +\infty]$
Normalized Mean Error (NME)	$NME = \frac{\sum_{i=1}^N M_i - O_i }{\sum_{i=1}^N O_i}$	$[0, +\infty]$
Root Mean Square Error (RMSE)	$RMSE = \left[\frac{1}{N} \sum_{i=1}^N (M_i - O_i)^2 \right]^{\frac{1}{2}}$	$[0, +\infty]$
Correlation Coefficient (R)	$R = \left\{ \frac{\sum_{i=1}^N (M_i - \bar{M})(O_i - \bar{O})}{\left[\sum_{i=1}^N (M_i - \bar{M})^2 \sum_{i=1}^N (O_i - \bar{O})^2 \right]^{\frac{1}{2}}} \right\}^{\frac{1}{2}}$	$[-1, 1]$

Note: $\bar{M} = \left(\frac{1}{N}\right) \sum_{i=1}^N M_i$, $\bar{O} = \left(\frac{1}{N}\right) \sum_{i=1}^N O_i$, M_i and O_i are values of model prediction and observation at time and location i , respectively. N is the number of samples.

Table 3
Performance statistics of simulated hourly ground-level O₃ concentrations in comparison with observations in Henan during 2015–2018.

Year	Mean Obs (ppm)	Mean Sim (ppm)	MB (ppm)	NMB (%)	NME (%)	RMSE (ppm)	R
Mean	0.048	0.046	-0.002	-5.0	45.0	0.030	0.5
2015	0.040	0.039	-0.001	-2.0	50.0	0.028	0.5
2016	0.047	0.047	0.00	1.0	47.0	0.033	0.5
2017	0.052	0.046	-0.006	-11.0	40.0	0.028	0.6
2018	0.053	0.049	-0.004	-7.0	44.0	0.032	0.6

observations of air temperature at 2 m above the ground (T2), wind speed (WS) and wind direction (WD) at 10 m above the ground, and the precipitation (PRE) at 129 meteorological stations in domain 2 (Fig. 1) during 2015–2018. The meteorological observation data were obtained from the National Oceanic and Atmospheric Administration (NOAA)--National Climatic Data Center Surface (NCDC). The simulated ozone concentrations were evaluated by using the hourly in situ observations of the O₃ concentrations at 83 observation sites in Henan. The ozone measurements were obtained from the China National Environmental Monitoring Center (<http://106.37.208.233:20035/>).

To evaluate the performance of the WRF/Chem model, the statistical indices were used here include Mean Bias (MB), Normalized Mean Error (NME), Normalized Mean Bias (NMB), Root Mean Square Error (RMSE), and Correlation Coefficient (R) (Zhang et al., 2006; Song et al., 2017). The calculation method description of these statistical indices can be referenced in Table 2. For more detailed information of these statistical indices, please refer to Zhang et al. (2006).

2.4. Calculation of AOT40 and losses of yield and economy

In this study, we adopted AOT40 to estimate the winter wheat yield loss in Henan during the growing seasons from 2015 to 2018. The AOT40 is the sum of hourly O₃ concentrations exceed 0.04 ppm (Dingenen et al., 2009; Zhao et al., 2018; Feng et al., 2019b):

$$AOT40 \text{ (ppm h)} = \sum_{i=1}^n ([O_3]_i - 0.04), [O_3]_i > 0.04 \text{ ppm} \quad (1)$$

where $[O_3]_i$ is the hourly O₃ concentration during daytime hours (Beijing time: 08:00–18:00). n is the total number of hours during growing seasons of winter wheat. It has been widely used in analysis of crop yield losses (Hu et al., 2020) due to it has been found to be closely related to the RYL of crops (Mills et al., 2007). The growing season was defined as a 75 days period from 44 days before to 30 days after the mid-anthesis date (Zhu et al., 2011). The map of mid-anthesis date was generated based on the observational crop datasets at 35 local agrometeorological

experimental stations provided by the Chinese Meteorological Service by using the universal kriging method of ArcGIS 10.6 software (Fig. S1). The hourly O₃ concentration at the ground surface (around 25 m) was obtained from the WRF/Chem model in this study, but the exposure height of wheat was around 1 m. The simulated ground level ozone concentrations should be converted to concentrations at 1 m height due to the vertical concentration gradient. Therefore, we adopted the method of Pleijel (1998) to convert the simulated ground level ozone concentration to 1 m height.

The AOT40 was commonly used as an exposure index for the assessment of the potential risk of the ground-level ozone to crops (Feng et al., 2019b; Hu et al., 2020; Zhao et al., 2020). It has been often used to assess impacts of ground-level O₃ on crops over the past two decades because it is closely correlated with the relative yield (RY) of crops such as wheat, maize, rice (Liu et al., 2009; Feng et al., 2012, 2019b; Wang et al., 2012; Zhu et al., 2015), etc. Here we adopted the AOT40-based response function parameterized by Zhu et al. (2011) in China to estimate the yield losses of winter wheat caused by surface O₃ exposure in Henan. Following is the calculation expression of the wheat relative yield (WRY):

$$WRY = -0.0205 \times AOT40 + 1 \quad (2)$$

The winter wheat relative yield losses (WRYL) was calculated based on the following expression:

$$WRYL = 1 - WRY \quad (3)$$

According to the calculation method of Zhao et al. (2020), we assessed the winter wheat production and economic losses by using the following formulas:

$$WPL = WRYL \times WP / (1 - WRYL) \quad (4)$$

$$EL = WPL \times WPP \quad (5)$$

where WPL is losses of wheat production. WP is the wheat production. EL is the economic loss of wheat induced by the ground-level ozone exposure. WPP is the minimum purchase price set by the Chinese government for wheat (<http://www.lswz.gov.cn/>). The WP datasets of 123 counties in Henan were obtained from the Statistical Yearbook of Henan, China (2015–2018) (<http://www.ha.stats.gov.cn/>). Fig. S2 shows the spatial and temporal variations of WP in Henan at the county level from 2015 to 2018.

3. Results

3.1. Performance of O₃ simulations

Meteorological conditions can directly affect the accuracy of O₃ simulation. Table S1 shows that WRF/Chem can provide well

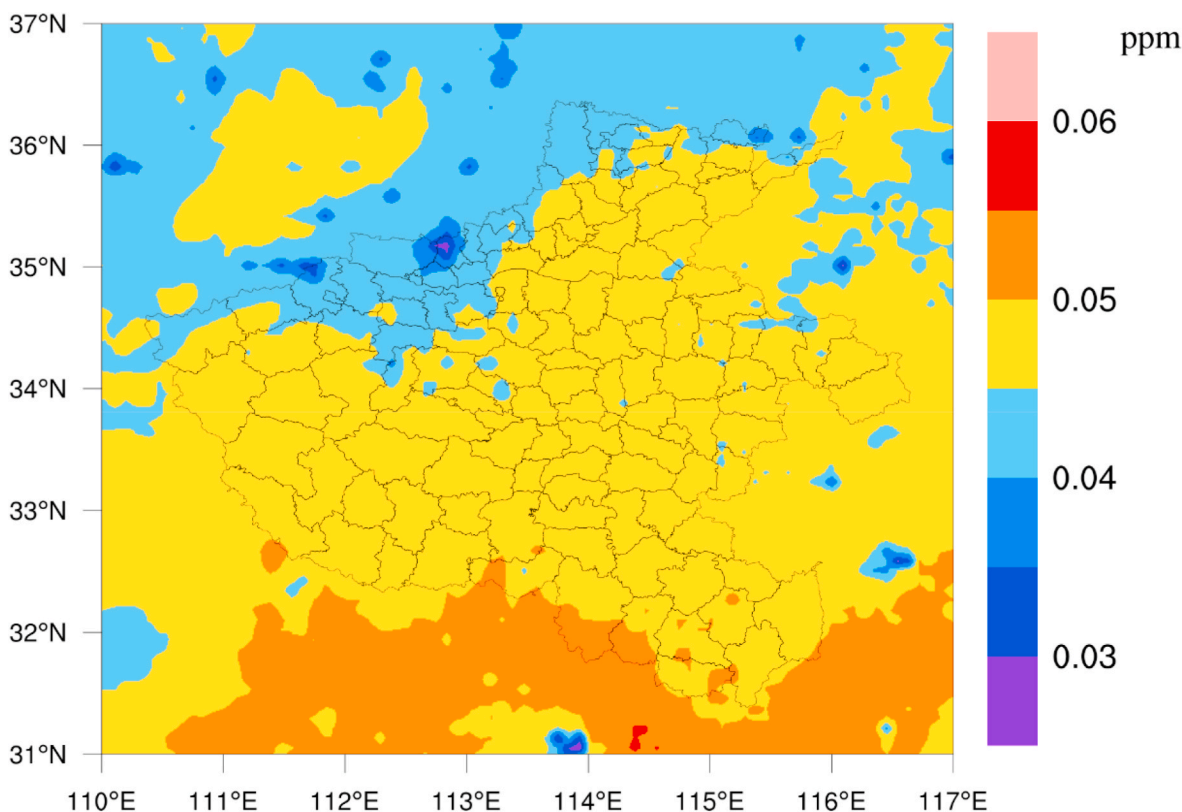


Fig. 2. The spatial distribution of annual mean O₃ concentration during 2015–2018.

meteorological variables during 2015–2018. To evaluate the performance of O₃ concentrations simulated by WRF/Chem, O₃ measurements (2015–2018) at 83 observational sites were adopted to compare with O₃ simulations. In general, the O₃ concentrations in Henan were relatively underpredicted (Table 3). The annual mean MB, NME, NMB, RMSE, and R of O₃ concentrations during 2015–2018 were −0.002 ppm, 45.0%, −5.0%, 0.030 ppm, and 0.5, respectively. The simulated O₃ concentrations in 2016 showed best performance compared with other three years. This may be due to the anthropogenic emission inventories of simulations during 2016–2018 was obtained from MEIC in 2016. Fig. S3 shows that the model performance at the 83 observational sites. Generally, we can see that the ozone simulation was better in northern regions than in southern regions. This could also mainly be attributed to the potential errors of anthropogenic emission inventories.

3.2. Spatiotemporal variations of ozone concentration and AOT40

The annual average O₃ concentration of Henan at daytime (8:00–18:00) during the wheat growing season were 0.049 ppm, 0.048 ppm, 0.051 ppm, and 0.052 ppm from 2015 to 2018, respectively. There were significant spatial and temporal variations in O₃ concentrations at the county level during 2015–2018 (Fig. 3). In general, the most severe regions of O₃ pollution mainly distributed in south of Henan during this period (> 0.05 ppm) (Fig. 2). The ground level O₃ concentrations in most counties of Henan showed an upward inter-annual variation during 2016–2018 (Fig. 3), especially some counties in northeast and southern Henan. The hourly O₃ concentrations at daytime during the wheat growing season exceeded 0.04 ppm in most counties (99.19% in 2015, 99.19% in 2016, 100% in 2017, and 100% in 2018). Fig. 4a shows the distribution of urban and rural areas in Henan. In most municipal regions, ozone concentrations were higher in urban areas than in rural areas (Fig. 4b), indicating that there were clearly differences in ozone concentrations between urban and rural areas.

The annual mean AOT40 during the wheat growing season in Henan

was 6.25 ppm h, 4.32 ppm h, 5.26 ppm h, and 6.87 ppm h from 2015 to 2018, respectively. Figs. 5a and 6 show that AOT40 had large spatial and temporal variations at the county level during 2015–2018. The counties with highest annual mean AOT40 (7.23–8.21 ppm h) were distributed in northeast of Henan (Fig. 5a), but the western and southeast counties had lower AOT40 (≤ 4.29 ppm h) than other counties. In 2015, the counties with highest AOT40 (> 8 ppm h) were mainly distributed in northeast Henan and the AOT40 in most counties was higher than in 2016 and 2017. The AOT40 was lowest (≤ 5 ppm h) over all the counties in 2016, but then it showed an increasing trend year by year until 2018 (Fig. 6). The AOT40 in some counties of northeastern Henan exceeded 8 ppm h (Fig. 6a, c, and d).

3.3. Wheat yield and economic losses

Figs. 5b and 7 show that there were large spatial and temporal variations in WRYL in Henan during the period of 2015–2018. In general, WRYL was higher in eastern than that in western Henan counties (Figs. 5b and 7) and the highest WRYL counties (14.8–16.8%) were distributed in northeast Henan (Fig. 5b). All counties had lowest WRYL in 2016 compared with other three years (Fig. 7), but WRYL over most counties has been increasing year by year since 2016. The WRYL in some counties of eastern Henan can be up to 15% or more in 2015, 2017, and 2018 (Fig. 7a, c, and d). Moreover, the WRYL exceeded 13% in most counties of Henan in 2018.

The mean WP was 3606.63×10^4 metric tons during 2015–2018 in Henan. The mean WPL and EL due to the ground level O₃ exposure were 509.91×10^4 metric tons (accounting for around 14% of the total wheat production) and 1825.73 million US dollars, respectively. The WPL and EL decreased in 2016 compared with them in 2015, but they showed an increasing inter-annual variation year by year from 2016 to 2018 (WPL: 371.24×10^4 metric tons (2016); 482.00×10^4 metric tons (2017); 621.68×10^4 metric tons (2018); EL: 1318.57 million US dollars (2016); 1683.03 million US dollars (2017); 2161.22 million US dollars (2018))

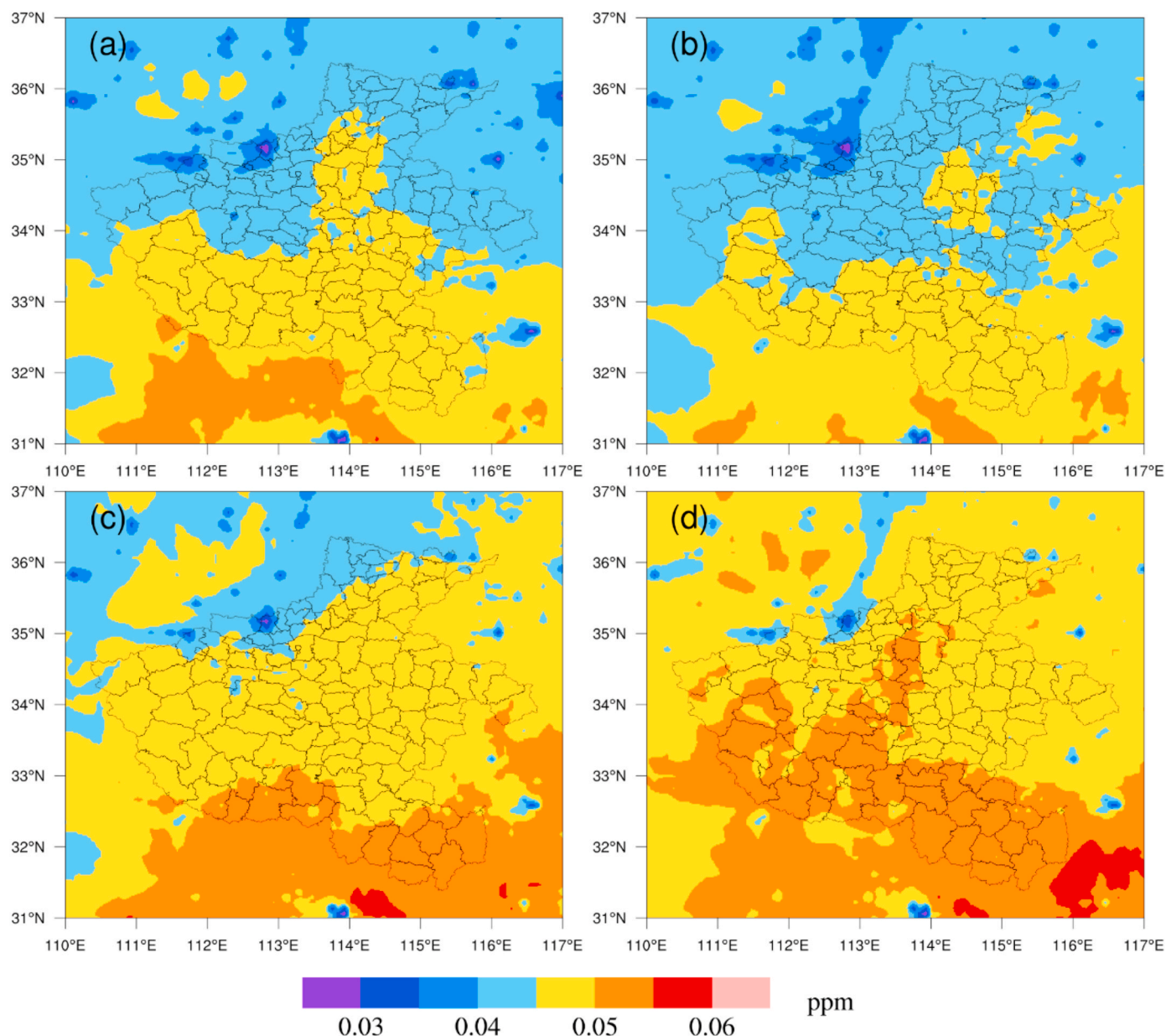


Fig. 3. Maps of average daytime (08:00–18:00) O_3 concentrations during wheat growing seasons in Henan from 2015 to 2018 (a, 2015; b, 2016; c, 2017; d, 2018).

(Fig. 8). Figs. S4 and S5 show the spatiotemporal variations of WPL and EL induced by the O_3 exposure at the county level during 2015–2018.

4. Discussion

Ground-level ozone has been used as one of the most primary air pollutants and its annual mean ground level O_3 has exceeded 0.04 ppm in many areas of the world (Paoletti et al., 2014; Zhao et al., 2018), causing severe negative impacts on crops production (Zhao et al., 2018, 2020; Hu et al., 2020) and showing a clearly upward trend over the past several decades (Gilge et al., 2010; Zhao et al., 2018; Liu et al., 2020). To quantify the impacts of O_3 pollution on crops, numerous studies have reported the evaluation of crops for yield and economic losses because the ground-level O_3 exposure (Lin et al., 2018; Zhao et al., 2018, 2020; Feng et al., 2019a, 2019b; Hu et al., 2020). The O_3 data adopted in these studies were mainly obtained from atmospheric chemistry transport models (Dingenen et al., 2009; Avnery et al., 2011b; Tang et al., 2013; Sicard et al., 2017; Lin et al., 2018) or O_3 observations (Zhao et al., 2018, 2020; Feng et al., 2019b).

The quality of O_3 data can directly determine the accuracy of the assessment of RYL induced by the ground-level O_3 exposure. Many studies have found that there are large spatial and temporal variations for O_3 concentrations in urban and rural/suburban regions (Dueñas et al., 2004; Xu et al., 2011; Guerreiro et al., 2014; Sicard et al., 2016, 2017). Although some studies adopted O_3 measurements to assess the impacts of ground-level O_3 pollution for crops yield losses, these studies may over-/under-estimate the crop yield losses due to the O_3 observation sites are often located in cities. The O_3 simulations based on atmospheric transport models, such as WRF/Chem, WRF/CMAQ, etc., still have uncertainties due to the uncertainties in emission inventories, meteorological simulations, or chemical mechanisms, but these models can capture the spatial and temporal disparities in urban and rural/suburban areas. The O_3 data adopted in this study were simulated by WRF/Chem model. The mean bias of the hourly O_3 simulations was -0.002 ppm, which indicated that WRF/Chem model can well simulated the hourly O_3 concentrations and be adopted to evaluate the impacts of surface ozone on losses of crop yields.

We found that the ground-level O_3 concentration in almost all

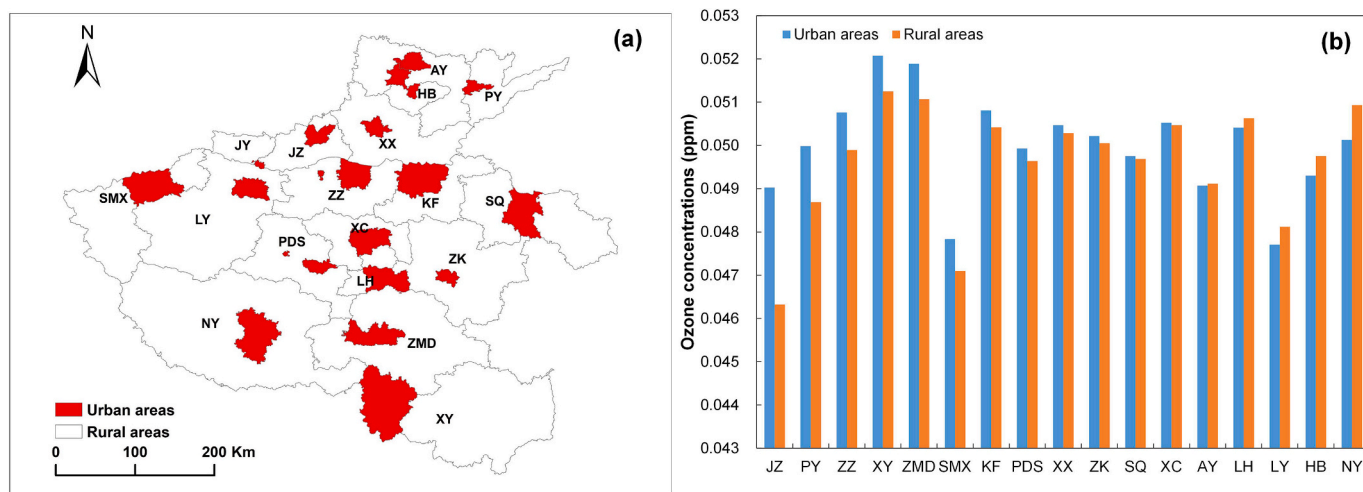


Fig. 4. Urban and rural regions map (a) and annual mean ozone concentration differences between urban and rural areas in Henan during 2015–2018 (b). The red shaded area is urban regions in Figs. (a). (JZ, Jiaozuo; PY, Puyang; ZZ, Zhengzhou; XY, Xinyang; ZMD, Zhumadian; SMX, Sanmenxia; KF, Kaifeng; PDS, Pingdingshan; XX, Xinxiang; ZK, Zhoukou; SQ, Shangqiu; XC, Xuchang; AY, Anyang; LH, Luohe; LY, Luoyang; HB, Hebi; NY, Nanyang). (For interpretation of the references to colour in this figure legend, the reader is referred to the Web version of this article.)

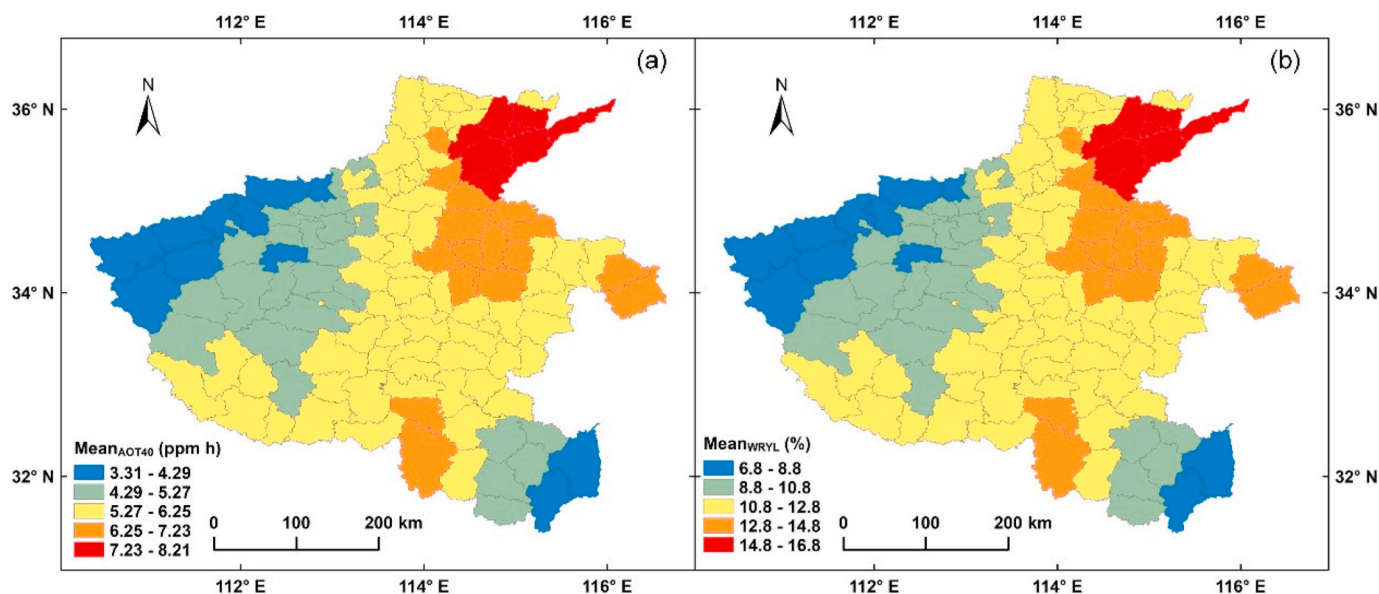


Fig. 5. Spatial distributions of mean AOT40 (a) and the relative yield loss of wheat (b) at the county level during 2015–2018.

counties of Henan has exceeded 0.04 ppm in the daytime during growing seasons from 2015 to 2018. In addition, the ground-level O₃ concentration represented an overall increasing trend in Henan during this period, which was consistent with previous studies (Lu et al., 2018; Zhao et al., 2020). The wheat production in Henan accounts for around 1/4 of the whole country, and it is a very important major grain production area in China. This indicated that the potential risks of the ground-level O₃ for crops in central China has become increasingly obvious in recent years. The AOT40 has been widely used as the exposure index that closely related to the losses of crop yields (Vingarzan, 2004; Zhao et al., 2018, 2020; Hu et al., 2020). Our annual AOT40 values ranged from 2 to 10 ppm h at the county level from 2015 to 2018, with the mean of 5.67 ppm h over Henan during this period. This result was relatively low compared with previous studies in regions of YRD and NCP and across China (Zhao et al., 2018; Feng et al., 2019b; Hu et al., 2020). This may be due to the fact that the O₃ concentration in Henan is lower than that in YRD, Beijing-Tianjin-Hebei region, and other regions

(Lin et al., 2018; Feng et al., 2019b). Although our results have some uncertainties, the AOT40 was more reasonable because it was calculated based on the mean value of the O₃ simulations within each county that takes into account the difference between urban and rural/suburban areas, rather than just using the measured O₃ data of urban monitoring stations.

In this study, we estimated WRYL and WPL based on the simulated AOT40 and the statistical WP at the county level in Henan, which can clearly show their spatial and temporal disparities. The county-level WRYL ranged from 4% to 21% during 2015–2018, with a mean of 12.8%, 8.8%, 10.8%, and 14.1% for the period of 2015–2018, respectively, which associated with WPL of 564.72×10^4 metric tons, 371.24×10^4 metric tons, 482.00×10^4 metric tons, and 621.68×10^4 metric tons, respectively. These simulated-based estimations of WRYL was comparable with those of previous studies over different regions.

Based on AOT40 response functions and measured/simulated O₃ data, several studies have reported the yield losses of crops caused by O₃

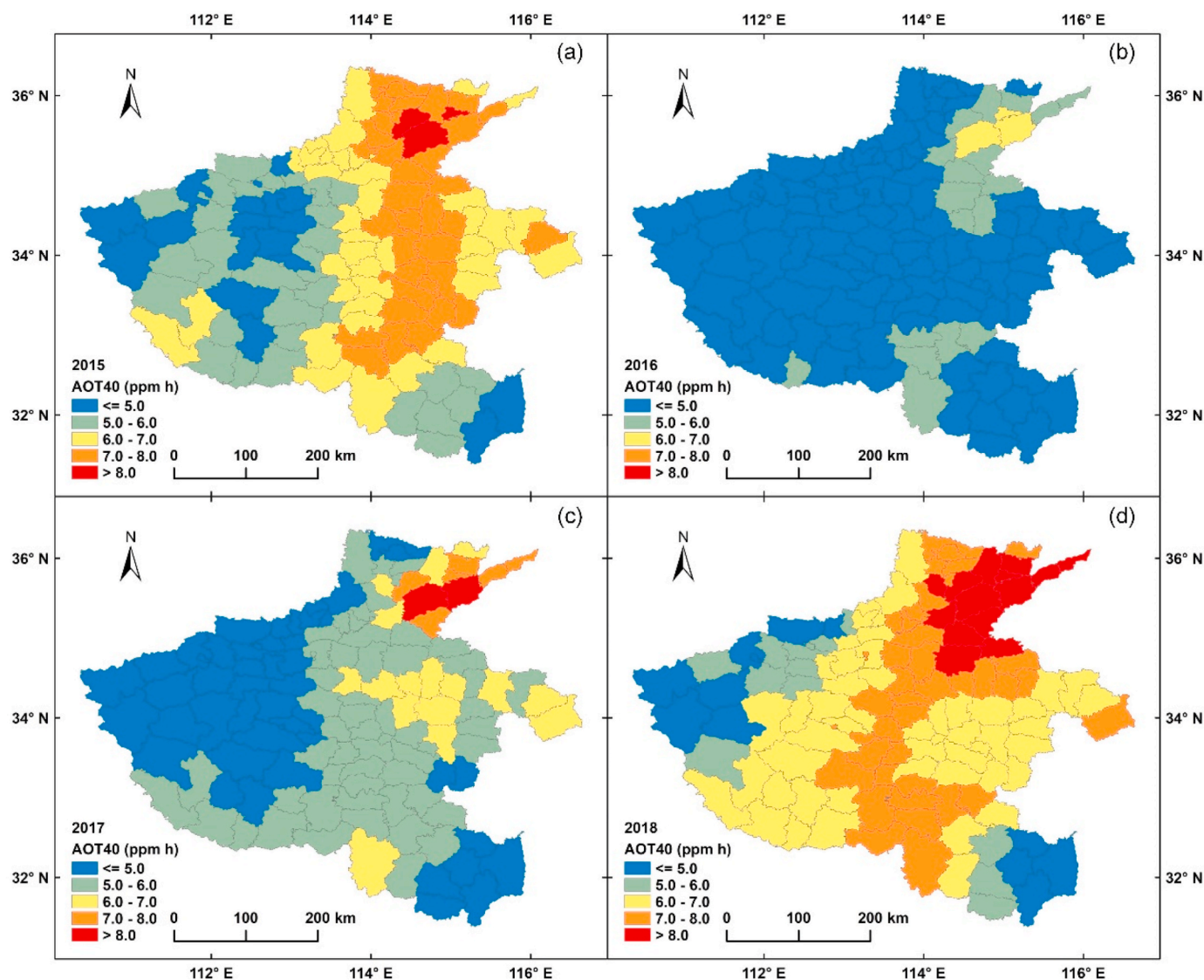


Fig. 6. Maps of AOT40 in Henan at the county level during the wheat growing season (a, 2015; b, 2016; c, 2017; d 2018).

exposure over different regions of China, such as NCP (17.1–30.8% during 2014–2017) (Feng et al., 2019b; Hu et al., 2020), YRD (26.4% in 2015) (Zhao et al., 2018), Chongqing (12% in 2000) (Liu et al., 2009), Northwest-Shandong Plain (12.9% in 2012) (Zhu et al., 2015), and across China (17.1% in 2015 and 18.1% in 2016) (Feng et al., 2019b). The simulated WRYL in this study was lower compared with some previous studies reported over Henan, such as the estimated mean WRYL of Henan was around 40% during 2015–2018 (Zhao et al., 2020) and 17.4% in 2016 (Feng et al., 2019b). This could be attributed to the differences between simulated and measured O_3 data, between the length of the accumulated period of AOT40, and between the slope of AOT40 response functions. The simulated O_3 data in this study were well consistent with measurements and can capture the difference between urban and rural areas. This may be more reasonable to describe the O_3 pollution level for each county, and then could reduce the uncertainty of the WRYL estimation. Zhao et al. (2018) took time window of 90 days as the accumulated period of AOT40, but the accumulated period of this study and Feng et al. (2019b) were the 44 days before and 30 days after the mid-anthesis date (75 days). This could explain why there was relatively lower WRYL in this study.

Results of this study provide useful information for understanding the potential effects of O_3 exposure on the winter wheat yield loss in

Henan—a major area of wheat production in China with severe O_3 pollution. However, there are still some uncertainties in this study. First, although WRF/Chem model can capture the difference of ozone between urban and rural/suburban areas, there still exist some uncertainties in the accuracy of O_3 concentration simulations due to the limitations of emission inventories. This may underestimate or overestimate the AOT40 and then affect the losses of wheat yields caused by O_3 pollution. To increase the accuracy of surface O_3 risk estimation, the spatial and temporal resolution of emission inventories should be improved and more rural O_3 measurement stations should be built in the future. Next, the O_3 -based response function could influence the accuracy of the WRYL estimation. The slope of the AOT40 response function adopted in this study may induce uncertainties for the assessment of WRYL due to it was parameterized by Zhu et al. (2011) based on OTC experiments in Jiangsu, China. In addition, the sensitivities of different cultivars to surface O_3 exposure are different (Fiscus et al., 2005). It is difficult to estimate the yield losses of crops for different cultivars induced by ground-level O_3 pollution because the scarce of experimental data for different cultivars in different regions of the world. Therefore, it is required to develop AOT40-response functions for the main cultivar of crop in specific regions. Third, the daytime window and the accumulated period for the calculation of AOT40 may cause some errors for

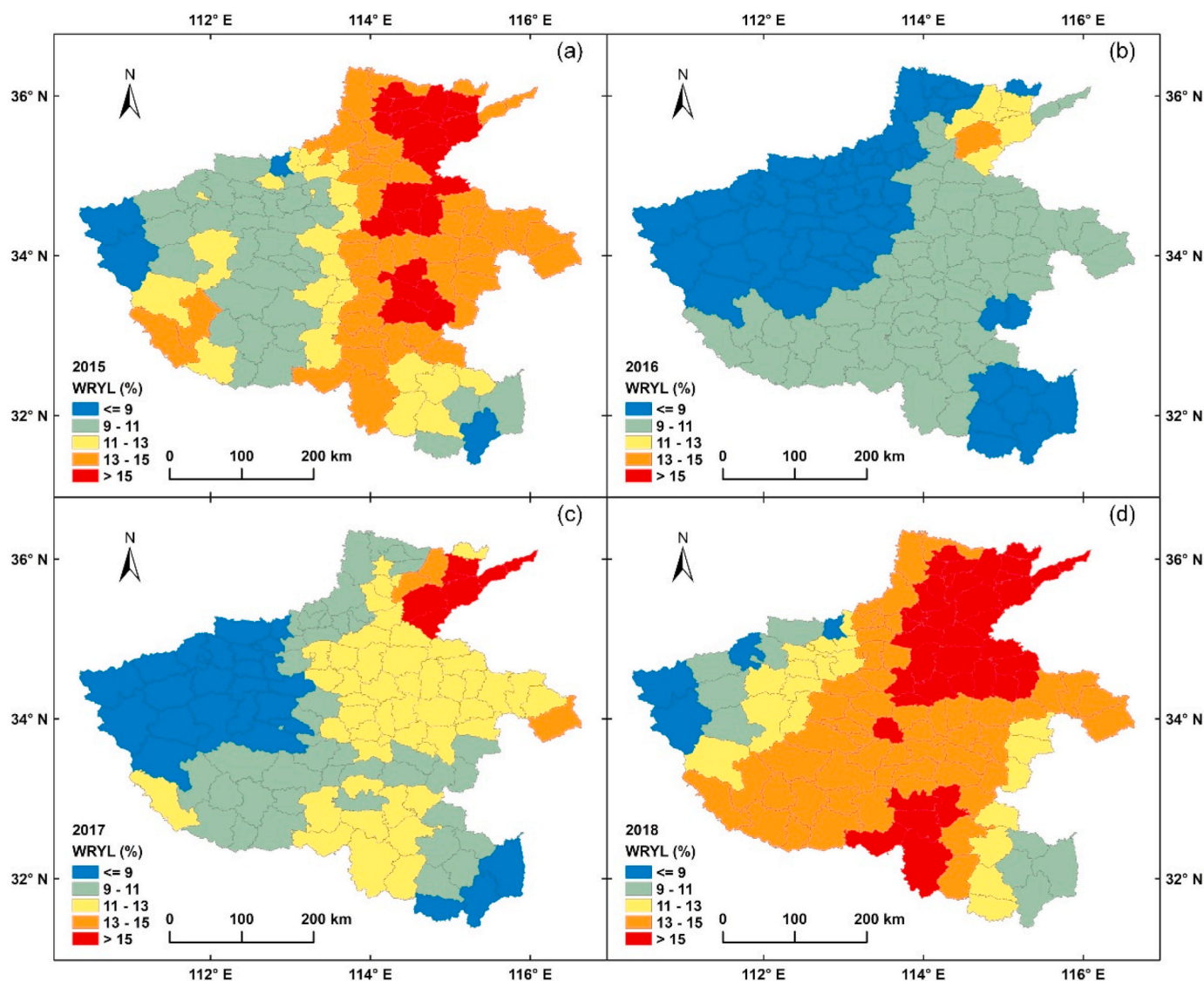


Fig. 7. Spatial distributions of relative yield loss of wheat in Henan at the county scale in 2015 (a), 2016 (b), 2017 (c), and 2018 (d).

WRYL assessment due to their difference over different regions, and thus the definition of daytime window and accumulated window for specific regions should be considered in the future. Compared with AOT40, PODy considered both ozone pollution and hydrothermal conditions during crop growing seasons. It can better explain the effect of ozone pollution on crop yield from the perspective of crop growth mechanisms. Therefore, the PODy metric should be considered to evaluate the effects of ozone pollution on crop yields. Moreover, the cultivated area of winter wheat was obtained from statistical data at the county level, which can also enhance the uncertainties in the estimation of yield losses caused by ozone pollution. The fine spatial distribution of winter wheat should be considered in the estimation of effects of ozone pollution on crop yield losses by using crop mapping algorithms based on remote sensing images (Pan et al., 2021a, 2021b) in the future.

5. Conclusions

In this study, we assessed the losses of yield and economy of winter wheat caused by O_3 exposure using WRF/Chem model simulated hourly ozone concentrations and the local AOT40-response functions in Henan of China during 2015–2018. We found that WRYL ranged from 4% to 21% in Henan. The mean wheat losses of relative yield and total

production was around 14% and 509.91×10^4 metric tons during the period of 2015–2018, respectively, and associated with economic loss of 1825.73 million US dollars. Although these results exist some uncertainty, it indicated that crops in China has been suffering high potential risk from the increasing surface O_3 exposure due to the increasing O_3 concentrations. Therefore, the government should propose more reasonable and stringent emission reduction measures to reduce the O_3 concentration levels and ensure food security.

CRedit authorship contribution statement

Tuanhui Wang: Software, Writing – original draft. **Lin Zhang:** Software, Data curation, Visualization. **Shenghui Zhou:** Software, Data curation. **Tianning Zhang:** Data curation, Visualization, Investigation. **Shiyan Zhai:** Data curation, Visualization, Investigation. **Zhongling Yang:** Validation, Writing – review & editing. **Dong Wang:** Validation, Writing – review & editing. **Hongquan Song:** Conceptualization, Supervision, Writing – review & editing, Funding acquisition.

Declaration of competing interest

The authors declare that they have no known competing financial

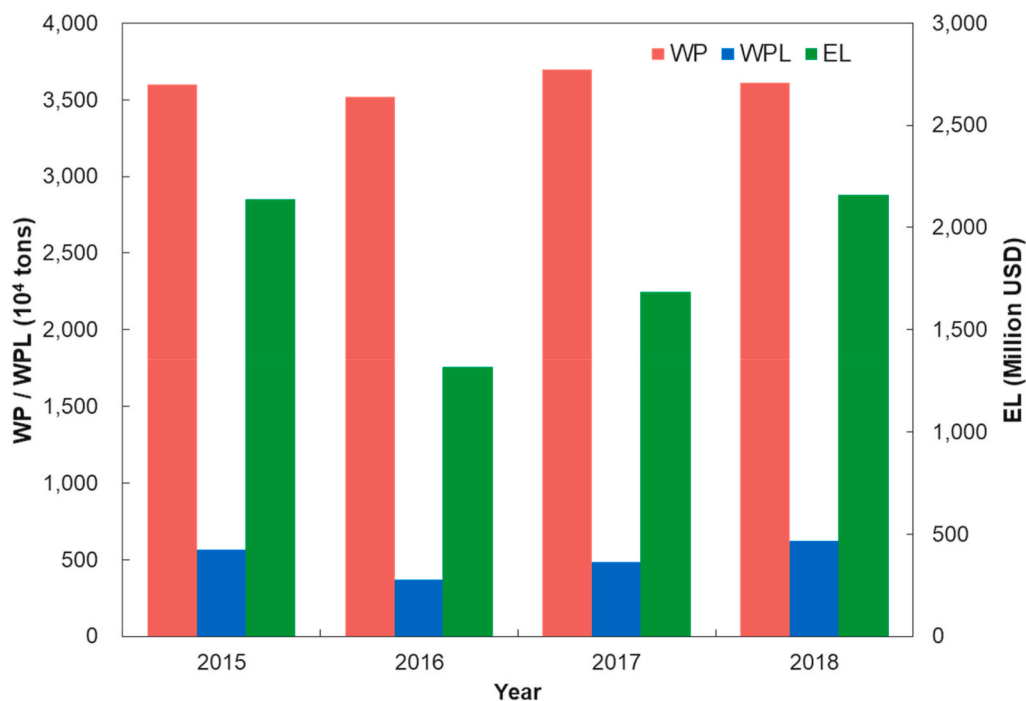


Fig. 8. Annual winter wheat production (WP), the wheat production losses (WPL), and economic losses (EL) of Henan from 2015 to 2018.

interests or personal relationships that could have appeared to influence the work reported in this paper.

Acknowledgements

This study was financially supported by the National Natural Science Foundation of China, China (41401107, 42071267) and the Support Plan for Science and Technology Innovation Team of Colleges and Universities in Henan, China (21IRTSTHN008). We the authors thank Chen Zhang and Chang Liu from Henan University, China for their help in data collection.

Appendix A. Supplementary data

Supplementary data to this article can be found online at <https://doi.org/10.1016/j.atmosenv.2021.118654>.

References

- Adams, R.M., Glycer, J.D., Johnson, S.L., McCarl, B.A., 1989. A reassessment of the economic effects of ozone on U.S. agriculture. *J. Air Waste Manag. Assoc.* 39, 960–968. <https://doi.org/10.1080/08940630.1989.10466583>.
- Amin, N., 2014. Effect of ozone on the relative yield of rice crop in Japan evaluated based on monitored concentrations. *Water Air Soil Pollut.* 225, 1797. <https://doi.org/10.1007/s11270-013-1797-5>.
- Avnery, S., Mauzerall, D.L., Liu, J., Horowitz, L.W., 2011a. Global crop yield reductions due to surface ozone exposure: 2. Year 2030 potential crop production losses, economic damage, and implications for world hunger under two scenarios of O₃ pollution. *Atmos. Environ.* 45 (13), 2297–2309. <https://doi.org/10.1016/j.atmosenv.2011.01.002>.
- Avnery, S., Mauzerall, D.L., Liu, J.F., Horowitz, L.W., 2011b. Global crop yield reductions due to surface ozone exposure: 1. Year 2000 crop production losses and economic damage. *Atmos. Environ.* 45 (13), 2284–2296. <https://doi.org/10.1016/j.atmosenv.2010.11.045>.
- Broberg, M.C., Feng, Z., Xin, Y., Pleijel, H., 2015. Ozone effects on wheat grain quality—A summary. *Environ. Pollut.* 197, 203–213. <https://doi.org/10.1016/j.envpol.2014.12.009>.
- Cai, S., Wang, Y., Zhao, B., Wang, S., Chang, X., Hao, J., 2017. The impact of the “air pollution prevention and control action plan” on PM_{2.5} concentrations in Jing-Jin-Ji region during 2012–2020. *Sci. Total Environ.* 580, 197–209. <https://doi.org/10.1016/j.scitotenv.2016.11.188>.
- Chen, F., Dudhia, J., 2001. Coupling an advanced land surface hydrology model with the Penn State NCAR MM5 modeling system. Part I: model implementation and

sensitivity. *Mon. Weather Rev.* 129, 569–585. [https://doi.org/10.1175/1520-0493\(2001\)129<0569:caalsh>2.0.co;2](https://doi.org/10.1175/1520-0493(2001)129<0569:caalsh>2.0.co;2).

- Cheng, L., Wang, S., Gong, Z., Li, H., Yang, Q., Wang, Y., 2018. Regionalization based on spatial and seasonal variation in ground-level ozone concentrations across China. *J. Environ. Sci.-China* 67, 179–190. <https://doi.org/10.1016/j.jes.2017.08.011>.
- Chou, M.D., Suarez, M.J., 1999. A solar radiation parameterization (CLIRAD-SW) for atmospheric studies. In: *NASA Tech. Memo. 10460*, vol. 15. NASA Goddard Space Flight Center, Greenbelt, MD, p. 48.
- Chou, M.D., Suarez, M.J., 1994. An efficient thermal infrared radiation parameterization for use in general circulation models. *NASA Tech. Memo.* 3, 85, 104606.
- Danh, N.T., Huy, L.N., Oanh, N.T.K., 2016. Assessment of rice yield loss due to exposure to ozone pollution in Southern Vietnam. *Sci. Total Environ.* 566–567, 1069–1079. <https://doi.org/10.1016/j.scitotenv.2016.05.131>.
- Debaje, S.B., 2014. Estimated crop yield losses due to surface ozone exposure and economic damage in India. *Environ. Sci. Pollut. Res.* 21 (12), 7329–7338. <https://doi.org/10.1007/s11356-014-2657-6>.
- Dingenen, R., Dentener, F.J., Raes, F., Krol, M.C., Emberson, L., Cofala, J., 2009. The global impact of ozone on agricultural crop yields under current and future air quality legislation. *Atmos. Environ.* 43, 604–618. <https://doi.org/10.1016/j.atmosenv.2008.10.033>.
- Dong, H., Chandratre, K., Qin, Y., Zhang, J., Tian, X., Rong, C., Wang, N., Guo, M., Zhao, G., Wang, S.M., 2020. Prevalence of BRCA1/BRCA2 pathogenic variation in Chinese Han population. *J. Med. Genet.* 1–5. <https://doi.org/10.1136/jmedgenet-2020-106970>, 0.
- Dueñas, C., Fernandez, M.C., Canete, S., Carretero, J., Liger, E., 2004. Analyses of ozone in urban and rural sites in Málaga (Spain). *Chemosphere* 56 (5), 631–639. <https://doi.org/10.1016/j.chemosphere.2004.04.013>.
- Feng, Z., De Marco, A., Anav, A., Gualtieri, M., Sicard, P., Tian, H., Fornasier, F., Tao, F., Guo, A., Paoletti, E., 2019a. Economic losses due to ozone impacts on human health, forest productivity and crop yield across China. *Environ. Int.* 131, 104966. <https://doi.org/10.1016/j.envint.2019.104966>.
- Feng, Z., Hu, E., Wang, X., Jiang, L., Liu, X., 2015. Ground-level O₃ pollution and its impacts on food crops in China: a review. *Environ. Pollut.* 199 (1), 42–48. <https://doi.org/10.1016/j.envpol.2015.01.016>.
- Feng, Z., Kobayashi, K., 2009. Assessing the impacts of current and future concentrations of surface ozone on crop yield with meta-analysis. *Atmos. Environ.* 43 (8), 1510–1519. <https://doi.org/10.1016/j.atmosenv.2008.11.033>.
- Feng, Z., Kobayashi, K., Li, P., Xu, Y., Tang, H., Guo, A., Paoletti, E., Calatayud, V., 2019b. Impacts of current ozone pollution on wheat yield in China as estimated with observed ozone, meteorology and day of flowering. *Atmos. Environ.* 116945. <https://doi.org/10.1016/j.atmosenv.2019.116945>.
- Feng, Z., Tang, H., Uddling, J., Pleijel, H., Kobayashi, K., Zhu, J., Oue, H., Guo, W., 2012. A stomatal ozone flux-response relationship to assess ozone-induced yield loss of winter wheat in subtropical China. *Environ. Pollut.* 164, 16–23. <https://doi.org/10.1016/j.envpol.2012.01.014>.
- Fiscus, E.L., Booker, F.L., Burkley, K.O., 2005. Crop responses to ozone: uptake, modes of action, carbon assimilation and partitioning. *Plant Cell Environ.* 28, 997–1011. <https://doi.org/10.1111/j.1365-3040.2005.01349.x>.

- Fuhrer, J., Skarby, L., Ashmore, M.R., 1997. Critical levels for ozone effects on vegetation in Europe. *Environ. Pollut.* 97, 91–106. [https://doi.org/10.1016/s0269-7491\(97\)00067-5](https://doi.org/10.1016/s0269-7491(97)00067-5).
- Gaudel, A., Cooper, O.R., Chang, K.L., Bourgeois, I., Ziemke, J.R., Strode, S.A., Oman, L. D., Sellitto, P., Nédélec, P., Blot, R., Thouret, V., Granier, C., 2020. Aircraft observations since the 1990s reveal increases of tropospheric ozone at multiple locations across the Northern Hemisphere. *Sci. Adv.* 6 <https://doi.org/10.1126/sciadv.aba8272> eaba8272.
- Ghude, S.D., Jena, C., Chate, D.M., Beig, G., Pfister, G.G., Kumar, R., Ramanathan, V., 2014. Reductions in India's crop yield due to ozone. *Geophys. Res. Lett.* 41 (15), 5685–5691. <https://doi.org/10.1002/2014gl060930>.
- Gilge, S., Plass-Duelmer, C., Fricke, W., Kaiser, A., Ries, L., Buchmann, B., Steinbacher, M., 2010. Ozone, carbon monoxide and nitrogen oxides time series at four alpine GAW mountain stations in central Europe. *Atmos. Chem. Phys.* 10, 12295–12316. <https://doi.org/10.5194/acp-10-12295-2010>.
- Grell, E., Grell, G., Bao, J.W., 2013. Experimenting with a convective parameterization scheme suitable for high-resolution mesoscale models in tropical cyclone simulations. *Geophys. Res. Abstr.* 15. EGU2013-5746-2.
- Grunhage, L., Pleijel, H., Mills, G., Bender, J., Danielsson, H., Lehmann, Y., Castell, J.F., Bethenod, O., 2012. Updated stomatal flux and flux-effect models for wheat for quantifying effects of ozone on grain yield, grain mass and protein yield. *Environ. Pollut.* 165, 147–157. <https://doi.org/10.1016/j.envpol.2012.02.026>.
- Guarin, J.R., Emberson, L., Simpson, D., Hernandez-Ochoa, I.M., Rowland, D., Asseng, S., 2019. Impacts of tropospheric ozone and climate change on Mexico wheat production. *Climatic Change* 155, 157–174. <https://doi.org/10.1007/s10584-019-02451-4>.
- Guenther, A., Karl, T., Harley, P., Wiedinmyer, C., Palmer, P.I., Geron, C., 2006. Estimates of global terrestrial isoprene emissions using MEGAN (model of emissions of gases and aerosols from nature). *Atmos. Chem. Phys.* 6 (11), 3181–3210. <https://doi.org/10.5194/acp-6-3181-2006>.
- Guo, H., Chen, K., Wang, P., Hu, J., Ying, Q., Gao, A., Zhang, H., 2019. Simulation of summer ozone and its sensitivity to emission changes in China. *Atmos. Pollut. Res.* 10, 1543–1552. <https://doi.org/10.1016/j.apr.2019.05.003>.
- Guerreiro, C.B.B., Foltescu, V., de Leeuw, F., 2014. Air quality status and trends in Europe. *Atmos. Environ.* 98, 376–384. <https://doi.org/10.1016/j.atmosenv.2014.09.017>.
- Hu, T., Liu, S., Xu, Y., Feng, Z., Calatayud, V., 2020. Assessment of O₃-induced yield and economic losses for wheat in the North China Plain from 2014 to 2017, China. *Environ. Pollut.* 258, 113828. <https://doi.org/10.1016/j.envpol.2019.113828>.
- Janjic, Z.I., 1994. The step-mountain eta coordinate model: further developments of the convection, viscous sublayer, and turbulence closure schemes. *Mon. Weather Rev.* 122 (5), 927–945. [https://doi.org/10.1175/1520-0493\(1994\)122h0927:TSMCEM2.0.CO;2](https://doi.org/10.1175/1520-0493(1994)122h0927:TSMCEM2.0.CO;2).
- Lal, S., Venkataramani, S., Naja, M., Kuniyal, J.C., Mandal, T.K., Bhuyan, P.K., Kumari, K. M., Tripathi, S.N., Sarkar, U., Das, T., Swamy, Y.V., Gopal, K.P., Gadhavi, H., Kumar, M.K.S., 2017. Loss of crop yields in India due to surface ozone: an estimation based on a network of observations. *Environ. Sci. Pollut. Res.* 24, 20972–20981. <https://doi.org/10.1007/s11356-017-9729-3>.
- Lamarque, J.F., Emmons, L.K., Hess, P.G., Kinnison, D.E., Tilmes, S., Vitt, F., Heald, C.L., Holland, E.A., Lauritzen, P.H., Neu, J., Orlando, J.J., Rasch, P.J., Tyndall, G.K., 2012. CAM-chem: description and evaluation of interactive atmospheric chemistry in the Community Earth System Model. *Geosci. Model Dev.* 5, 369–411. <https://doi.org/10.5194/gmd-5-369-2012>.
- Lapina, K., Henze, D.K., Milford, J.B., Travis, K., 2016. Impacts of foreign, domestic, and state-level emissions on ozone-induced vegetation loss in the United States. *Environ. Sci. Technol.* 50, 806–813. <https://doi.org/10.1021/acs.est.5b04887>.
- Li, K., Jacob, D.J., Shen, L., Lu, X., De Smedt, I., Liao, H., 2020. Increases in surface ozone pollution in China from 2013 to 2019: anthropogenic and meteorological influences. *Atmos. Chem. Phys.* 20, 11423–11433. <https://doi.org/10.5194/acp-20-11423-2020>.
- Li, P., De Marco, A., Feng, Z., Anav, A., Zhou, D., Paoletti, E., 2018. Nationwide ground-level ozone measurements in China suggest serious risks to forests. *Environ. Pollut.* 237, 803–813. <https://doi.org/10.1016/j.envpol.2017.11.002>.
- Li, X., Song, H., Zhai, S., Lu, S., Kong, Y., Xia, H., Zhao, H., 2019. Particulate matter pollution in Chinese cities: areal-temporal variations and their relationships with meteorological conditions (2015–2017). *Environ. Pollut.* 246, 11–18. <https://doi.org/10.1016/j.envpol.2018.11.103>.
- Lin, Y., Jiang, F., Zhao, J., Zhu, G., He, X., Ma, X., Li, S., Sabel, C.E., Wang, H., 2018. Impacts of O₃ on premature mortality and crop yield loss across China. *Atmos. Environ.* <https://doi.org/10.1016/j.atmosenv.2018.09.024>.
- Lin, Y.L., Farley, R.D., Orville, H.D., 1983. Bulk parameterization of the snow field in a cloud model. *J. Clim. Appl. Meteorol.* 22, 1065–1092. [https://doi.org/10.1175/1520-0450\(1983\)022<1065:BPOTSF>2.0.CO;2](https://doi.org/10.1175/1520-0450(1983)022<1065:BPOTSF>2.0.CO;2).
- Liu, F., Wang, X., Zhu, Y., 2009. Assessing current and future ozone-induced yield reductions for rice and winter wheat in Chongqing and the Yangtze River Delta of China. *Environ. Pollut.* 157 (2), 707–709. <https://doi.org/10.1016/j.envpol.2008.09.012>.
- Liu, P., Song, H., Wang, T., Wang, F., Li, X., Miao, C., Zhao, H., 2020. Effects of meteorological conditions and anthropogenic precursors on ground-level ozone concentrations in Chinese cities. *Environ. Pollut.* 262, 114366. <https://doi.org/10.1016/j.envpol.2020.114366>.
- Liu, X.H., Zhang, Y., Xing, J., Zhang, Q., Wang, K., Streets, D.G., Jang, C., Wang, W.X., Hao, J.M., 2010. Understanding of regional air pollution over China using CMAQ, part II. Process analysis and sensitivity of ozone and particulate matter to precursor emissions. *Atmos. Environ.* 44, 3719–3727. <https://doi.org/10.1016/j.atmosenv.2010.03.036>.
- Lu, X., Hong, J., Zhang, L., Cooer, O.R., Schultz, M.G., Xu, X., Wang, T., Gao, M., Zhao, Y., Zhang, Y., 2018. Severe surface ozone pollution in China: a global perspective. *Environ. Sci. Technol. Lett.* 5, 487–494. <https://doi.org/10.1021/acs.estlett.8b00366>.
- Madronich, S., 1987. Intercomparison of NO₂ photodissociation and u.v. radiometer measurements. *Atmos. Environ.* 21, 569–578. [https://doi.org/10.1016/0004-6981\(87\)90039-4](https://doi.org/10.1016/0004-6981(87)90039-4).
- Massman, W.J., Musselman, R.C., Lefohn, A.S., 2000. A conceptual ozone dose-response model to develop a standard to protect vegetation. *Atmos. Environ.* 34 (5), 745–759. [https://doi.org/10.1016/s1352-2310\(99\)00395-7](https://doi.org/10.1016/s1352-2310(99)00395-7).
- McGrath, J.M., Betzelberger, A.M., Wang, S., Shook, E., Zhu, X.G., Long, S.P., Ainsworth, E.A., 2015. An analysis of ozone damage to historical maize and soybean yields in the United States. *P. Natl. Acad. Sci. USA.* 112 (46), 14390–14395. <https://doi.org/10.1073/pnas.1509777112>.
- Mills, G., Pleijel, H., Braun, S., Buker, P., Bermejo, V., Calvo, E., Danielsson, H., Emberson, L., Fernandez, I.G., Grunhage, L., Harmens, H., Hayes, F., Karlsson, P.E., Simpson, D., 2011. New stomatal flux-based critical levels for ozone effects on vegetation. *Atmos. Environ.* 45 (28), 5064–5068. <https://doi.org/10.1016/j.atmosenv.2011.06.009>.
- Mills, G., Buse, A., Gimeno, B., Bermejo, V., Holland, M., Emberson, L., Pleijel, H., 2007. A synthesis of AOT40-based response functions and critical levels of ozone for agricultural and horticultural crops. *Atmos. Environ.* 41, 2630–2643. <https://doi.org/10.1016/j.atmosenv.2006.11.016>.
- Mills, G., Pleijel, H., Malley, C.S., Sinha, B., Cooper, O.R., Schultz, M.G., Neufeld, H.S., Simpson, D., Sharps, K., Feng, Z., Gerosa, G., Harmens, H., Kobayashi, K., Saxena, P., Paoletti, E., Sinha, V., Xu, X., 2018a. Tropospheric Ozone Assessment Report: present-day tropospheric ozone distribution and trends relevant to vegetation. *Elem. Sci. Anth.* 6, 47. <https://doi.org/10.1525/elementa.302>.
- Mills, G., Sharps, K., Simpson, D., Pleijel, H., Broberg, M., Uddling, J., Jaramillo, F., J. Davies, W., Dentener, F., Van den Berg, M., Agrawal, M., Agrawal, S., Ainsworth, E., Buker, P., Emberson, L., Feng, Z., Harmens, H., Hayes, F., Kobayashi, K., Paoletti, E., Van Dingenen, R., 2018b. Ozone pollution will compromise efforts to increase global wheat production. *Global Change Biol.* 24 (8), 3560–3574. <https://doi.org/10.1111/gcb.14157>.
- Musselman, R.C., Lefohn, A.S., Massman, W.J., Heath, R., 2006. A critical review and analysis of the use of exposure- and flux-based ozone indices for predicting vegetation effects. *Atmos. Environ.* 40, 1869–1888. <https://doi.org/10.1016/j.atmosenv.2005.10.064>.
- Pan, L., Xia, H., Yang, J., Niu, W., Wang, R., Song, H., Guo, Y., Qin, Y., 2021a. Mapping cropping intensity in Huaihe basin using phenology algorithm, all Sentinel-2 and Landsat images in Google Earth Engine. *Int. J. Appl. Earth Obs.* 102, 102376. <https://doi.org/10.1016/j.jag.2021.102376>.
- Pan, L., Xia, H., Zhao, X., Guo, Y., Qin, Y., 2021b. Mapping winter crops using a phenology algorithm, time-series Sentinel-2 and Landsat-7/8 images, and Google Earth Engine. *Rem. Sens.* 13, 2510. <https://doi.org/10.3390/rs13132510>.
- Paoletti, E., De Marco, A., Beddows, D.C.S., Harrison, R.M., Manning, W.J., 2014. Ozone levels in European and USA cities are increasing more than at rural sites, while peak values are decreasing. *Environ. Pollut.* 192, 295–299. <https://doi.org/10.1016/j.envpol.2014.04.040>.
- Pleijel, H., 1998. A suggestion of a simple transfer function for the use of ozone monitoring data in dose-response relationships obtained using open-top chambers. *Water Air Soil Pollut.* 102, 61–74. <https://doi.org/10.1023/A:1004970227678>.
- Pleijel, H., Broberg, M.C., Uddling, J., Mills, G., 2018. Current surface ozone concentrations significantly decrease wheat growth, yield and quality. *Sci. Total Environ.* 613–614, 687–692. <https://doi.org/10.1016/j.scitotenv.2017.09.111>.
- Sicard, P., Anav, A., De Marco, A., Paoletti, E., 2017. Projected global ground-level ozone impacts on vegetation under different emission and climate scenarios. *Atmos. Chem. Phys.* 17, 12177–12196. <https://doi.org/10.5194/acp-17-12177-2017>.
- Sicard, P., Serra, R., Rossello, P., 2016. Spatiotemporal trends in ground-level ozone concentrations and metrics in France over the time period 1999–2012. *Environ. Res.* 149, 122–144. <https://doi.org/10.1016/j.envres.2016.05.014>.
- Singh, A.A., Agrawal, S.B., 2016. Tropospheric ozone pollution in India: effects on crop yield and product quality. *Environ. Sci. Pollut. Res.* 24 (5), 4367–4382. <https://doi.org/10.1007/s11356-016-8178-8>.
- Sinha, B., Singh-Sangwan, K., Maurya, Y., Kumar, V., Sarkar, C., Chandra, B.P., Sinha, V., 2015. Assessment of crop yield losses in Punjab and Haryana using 2 years of continuous in situ ozone measurements. *Atmos. Chem. Phys.* 15, 9555–9576. <https://doi.org/10.5194/acp-15-9555-2015>.
- Song, H., Wang, K., Zhang, Y., Hong, C., Zhou, S., 2017. Simulation and evaluation of dust emissions with WRF-Chem (v3.7.1) and its relationship to the changing climate over East Asia from 1980 to 2015. *Atmos. Environ.* 167, 511–522. <https://doi.org/10.1016/j.atmosenv.2017.08.051>.
- Tang, H., Takigawa, M., Liu, G., Zhu, J., Kobayashi, K., 2013. A projection of ozone-induced wheat production loss in China and India for the years 2000 and 2020 with exposure-based and flux-based approaches. *Global Change Biol.* 19, 2739–2752. <https://doi.org/10.1111/gcb.12252>.
- Tilmes, S., Lamarque, J.F., Emmons, L.K., Kinnison, D.E., Ma, P.L., Liu, X., Ghan, S., Bardeen, C., Arnold, S., Deeter, M., Vitt, F., Ryerson, T., Elkins, J.W., Moore, F., Spackman, J.R., Val Martin, M., 2015. Description and evaluation of tropospheric chemistry and aerosols in the community earth system model (CESM1.2). *Geosci. Model Dev.* 8, 1395–1426. <https://doi.org/10.5194/gmd-8-1395-2015>.
- Vingarzan, R., 2004. A review of surface ozone background levels and trends. *Atmos. Environ.* 38 (21), 3431–3442. <https://doi.org/10.1016/j.atmosenv.2004.03.030>.
- Wang, P., Chen, Y., Hu, J., Zhang, H., Ying, Q., 2019. Attribution of tropospheric ozone to NO_x and VOC emissions: considering ozone formation in the transition regime. *Environ. Sci. Technol.* 53, 1404–1412. <https://doi.org/10.1021/acs.est.8b05981>.

- Wang, T., Song, H., Wang, F., Zhai, S., Han, Z., Wang, D., Li, X., Zhao, H., Ma, R., Zhang, G., 2020. Hysteretic effects of meteorological conditions and their interactions on particulate matter in Chinese cities. *J. Clean. Prod.* 274, 122926. <https://doi.org/10.1016/j.jclepro.2020.122926>.
- Wang, T., Xue, L., Brimblecombe, P., Lam, Y.F., Li, L., Zhang, L., 2017. Ozone pollution in China: a review of concentrations, meteorological influences, chemical precursors, and effects. *Sci. Total Environ.* 575, 1582–1596. <https://doi.org/10.1016/j.scitotenv.2016.10.081>.
- Wang, X., Manning, W., Feng, Z., Zhu, Y., 2007. Ground-level ozone in China: distribution and effects on crop yields. *Environ. Pollut.* 147, 394–400. <https://doi.org/10.1016/j.envpol.2006.05.006>.
- Wang, X., Zhang, Q., Zheng, F., Zheng, Q., Yao, F., Chen, Z., Zhang, W., Hou, P., Feng, Z., Song, W., Feng, Z., Lu, F., 2012. Effects of elevated O₃ concentration on winter wheat and rice yields in the Yangtze River Delta, China. *Environ. Pollut.* 171 (1), 118–125. <https://doi.org/10.1016/j.envpol.2012.07.028>.
- Watanabe, T., Izumi, T., Matsuyama, H., 2016. Accumulated phytotoxic ozone dose estimation for deciduous forest in Kanto, Japan in summer. *Atmos. Environ.* 129, 176–185. <https://doi.org/10.1016/j.atmosenv.2016.01.016>.
- Wiedinmyer, C., Yokelson, R.J., Gullett, B.K., 2014. Global emissions of trace gases, particulate matter, and hazardous air pollutants from open burning of domestic waste. *Environ. Sci. Technol.* 48 (16), 9523–9530. <https://doi.org/10.1021/es502250z>.
- Wilkinson, S., Mills, G., Illidge, R., Davies, W.J., 2012. How is ozone pollution reducing our food supply? *J. Exp. Bot.* 63 (2), 527–536. <https://doi.org/10.1093/jxb/err317>.
- Xu, J., Zhang, X., Xu, X., Zhao, X., Meng, W., Pu, W., 2011. Measurement of surface ozone and its precursors in urban and rural sites in Beijing. *Proc. Earth Planet. Sci.* 2, 255–261. <https://doi.org/10.1016/j.proeps.2011.09.041>.
- Yamaguchi, M., Hoshino, D., Inada, H., Akhtar, N., Sumioka, C., Takeda, K., Izuta, T., 2014. Evaluation of the effects of ozone on yield of Japanese rice (*Oryza sativa* L.) based on stomatal ozone uptake. *Environ. Pollut.* 184 (1), 472–480. <https://doi.org/10.1016/j.envpol.2013.09.024>.
- Yu, Y., Xu, H., Jiang, Y., Chen, F., Cui, X., He, J., Liu, D., 2021. A modeling study of PM_{2.5} transboundary transport during a winter severe haze episode in southern Yangtze River Delta, China. *Atmos. Res.* 248, 105159. <https://doi.org/10.1016/j.atmosres.2020.105159>.
- Zaveri, R.A., Easter, R.C., Fast, J.D., Peters, L.K., 2008. Model for simulating aerosol interactions and chemistry (MOSAIC). *J. Geophys. Res.* 113, D13204. <https://doi.org/10.1029/2007jd008782>.
- Zaveri, R.A., Peters, L.K., 1999. A new lumped structure photochemical mechanism for large-scale applications. *J. Geophys. Res.* 104 (D23), 30387–30415. <https://doi.org/10.1029/1999jd900876>.
- Zhai, Y., Zhang, T., Bai, Y., Ji, C., Ma, X., Shen, X., Hong, J., 2021. Energy and water footprints of cereal production in China. *Resour. Conserv. Recycl.* 164, 105150. <https://doi.org/10.1016/j.resconrec.2020.105150>.
- Zhang, Q., Streets, D.G., Carmichael, G.R., He, K.B., Huo, H., Kannari, A., Klimont, Z., Park, I.S., Reddy, S., Fu, J.S., Chen, D., Duan, L., Lei, Y., Wang, L.T., Yao, Z.L., 2009. Asian emissions in 2006 for the NASA INTEX-B mission. *Atmos. Chem. Phys.* 9, 5131–5153. <https://doi.org/10.5194/acp-9-5131-2009>.
- Zhang, Y., Liu, P., Pun, B., Seigneur, C., 2006. A comprehensive performance evaluation of MM5-CMAQ for the Summer 1999 Southern Oxidants Study episode-Part I: evaluation protocols, databases, and meteorological predictions. *Atmos. Environ.* 40 (26), 4825–4838. <https://doi.org/10.1016/j.atmosenv.2005.12.043>.
- Zhang, T., He, W., Zheng, H., Cui, Y., Song, H., Fu, S., 2021. Satellite-based ground PM_{2.5} estimation using a gradient boosting decision tree. *Chemosphere* 268, 128801. <https://doi.org/10.1016/j.chemosphere.2020.128801>.
- Zhao, H., Zheng, Y., Wu, X., 2018. Assessment of yield and economic losses for wheat and rice due to ground-level O₃ exposure in the Yangtze River Delta, China. *Atmos. Environ.* 191, 241–248. <https://doi.org/10.1016/j.atmosenv.2018.08.019>.
- Zhao, H., Zheng, Y., Zhang, Y., Li, T., 2020. Evaluating the effects of surface O₃ on three main food crops across China during 2015–2018. *Environ. Pollut.* 258, 113794. <https://doi.org/10.1016/j.envpol.2019.113794>.
- Zhu, X., Feng, Z., Sun, T., Liu, X., Tang, H., Zhu, J., Guo, W., Kobayashi, K., 2011. Effects of elevated ozone concentration on yield of four Chinese cultivars of winter wheat under fully open-air field conditions. *Global Change Biol.* 17 (8), 2697–2706. <https://doi.org/10.1111/j.1365-2486.2011.02400.x>.
- Zhu, Z., Sun, X., Zhao, F., Meixner, F.X., 2015. Ozone concentrations, flux and potential effect on yield during wheat growth in the Northwest-Shandong plain of China. *J. Environ. Sci.* 34 (8), 1–9. <https://doi.org/10.1016/j.jes.2014.12.022>.